Journal of. Modern Trends in Physics Research
Online ISSN 2636-4220
DOI: 10.19138/mtpr/(14)65-72
Accepted: 2014-12-19

Effect of blending ratio and Carbon concentration on the stress-strain characteristics for NR/SBR Rubber

A. S. Abdel-Rahman, M. H. Soleiman, H. H. Hassan, S. S. Abdel-Aziz

Physics Department, Faculty of Science, Cairo University, Giza, Egypt.

Abstract- Blends of Natural Rubber/Styrene Butadiene Rubber (NR/SBR) loaded with different ratios of N220 carbon black filler were prepared. The mechanical properties of pure blends and those loaded with different ratios of carbon black were investigated. The (50NR/50SBR), 40N220/(50NR/50SBR) blends were found to exhibit the highest values of tensile strength and elongation at break. The theoretical Mooney-Rivlin model was applied to NR/SBR and supports the result of stress-strain characteristics. The values of shore hardness (A) for all samples were measured and showed a marked increase by increasing the black content.

Correspondence Author – scholar.cu.edu.eg/?q=asabry & asabry@sci.cu.edu.eg

Keywords- Carbon black; NR rubber; SBR rubber; stress; strain.

1. INTRODUCTION

Blending two or more polymers to produce new materials with mixed properties has been extensively developed in several industries [Alsuhaiqi *et al.* (2014); Nair *et al.* (2004)]. Natural rubber NR crystallizes under stretching, so that it resists deformation and enhances its strength while many synthetic rubbers such as styrene butadiene rubber SBR-1502 does not crystallize. Mixtures of NR and SBR are quite often used in order to get desired technological properties [Nair *et al.* (2004); El-Lawindy (2002)].

Carbon black is a widely used as a filler to enhance the performance of rubbers and other polymeric materials [Geyou *et al.* (2008)]. The reinforcement of elastomers by particulate fillers has been studied in depth in numerous investigations [Hajji *et al.* (1999); An and Jeong (2013)], and it is generally accepted that this phenomenon is, to a large extent, dependant on the physical interactions between the filler and the rubber matrix. The structure, surface characteristics and especially particle size of the fillers are the main factors that determine their reinforcing effects of composites [Zhou *et al.* (2007)].

The classical kinetic theory of rubber elasticity originally developed by Wall [1943], Flory [1953] and James and Guth [1943] attributed the high elasticity of a cross-liked rubber to the change of the conformational entropy of long flexible molecular chains.

Mooney [1940] and Rivlin [1948] theoretical approaches can describe the filler free blends according to relation plots true stress (σ) and elongation (λ) in Gaussian region, while Vand [1948] and Guth [1945] introduce relation for filler volume concentration applied in case of carbon loaded samples.

In the present work, mechanical properties of pure NR/SBR blends and those loaded with different ratios of two types of carbon blacks were studied. Mixed ratios of carbon black were also added to the rubber optimum blend in order to show the optimum values of mechanical properties, based on the theoretical models. The stress-strain curves were fitted to theoretical equations to discuss the density of cross-links and its dependence on the blend ratio.

Journal of. Modern Trends in Physics Research
Online ISSN 2636-4220
DOI: 10.19138/mtpr/(14)65-72
Accepted: 2014-12-19

2. Experimental

2.1. *Materials*

The samples under investigation were divided into three main groups:

2.1.1. *Carbon free samples*

They are denoted by NS and refer to the rubber blend of NR and SBR-1502 with different ratios. The compounding formulations (recipes) of composites are listed in table 1.

Table 1. The compounding recipe of the NS blends.

Ingredients (phr)[1]	NS01	NS19	NS28	NS37	NS46	NS55	NS64	NS73	NS82	NS91	NS10
NR	0	10	20	30	40	50	60	70	80	90	100
SBR-1502	100	90	80	70	60	50	40	30	20	10	0
Stearic acid	2	2	2	2	2	2	2	2	2	2	2
ZnO	5	5	5	5	5	5	5	5	5	5	5
Processing Oil	10	10	10	10	10	10	10	10	10	10	10
MBTS[2]	2	2	2	2	2	2	2	2	2	2	2
IPPD 4020[3]	1	1	1	1	1	1	1	1	1	1	1
Sulfur	2	2	2	2	2	2	2	2	2	2	2

[1]Part per hundred parts of rubber by weight in grams.
[2]MBTS methylebenzthiazyle disulfide (accelerator)
[3]IPPD 4020 N-isopropyl-N'-phenyl-p-phenylene diamine (antioxidant, antiozonant and antiflex)

2.1.2. *Carbon loaded samples*

The optimum sample (NS55) was loaded with (N220) black to form NS55N2. It was studies with concentration increment of 10 phr of carbon black (Table 2). The terms N2 refer to N220 black, and the carbon concentration in phr appears at the end of blend name.

Table 2. The compounding recipe of the NS55N2 Samples.

Ingredients (phr)	NS55N2L10	NS55N2L20	NS55N2L30	NS55N2L40	NS55N2L50	NS55N2L60	NS55N2L70	NS55N2L80	NS55N2L90	NS55N2L10(0
NR	50	50	50	50	50	50	50	50	50	50
SBR-1502	50	50	50	50	50	50	50	50	50	50
Stearic acid	2	2	2	2	2	2	2	2	2	2
ZnO	5	5	5	5	5	5	5	5	5	5
Processing Oil	10	10	10	10	10	10	10	10	10	10
N220	10	20	30	40	50	60	70	80	90	100
MBTS	2	2	2	2	2	2	2	2	2	2
IPPD 4020	1	1	1	1	1	1	1	1	1	1
Sulfur	2	2	2	2	2	2	2	2	2	2

2.2. *Samples preparation*

All rubber compounds were mixed according to the ASTM D 3182 [2012] standard by using a two-roll mill of 300 mm length, 150 mm diameter, speed of slow roll 18 rpm and gear ratio 1.4. The compounded rubbers were molded into dumbbell-shaped specimens of 2 mm thick, 7 mm width, and 100 mm length.

The vulcanization process was carried out by using an electrically heated platen press at 143±2°C and 15 MPa for 30 min.

Journal of. Modern Trends in Physics Research
Online ISSN 2636-4220
DOI: 10.19138/mtpr/(14)65-72
Accepted: 2014-12-19

2.3. *Mechanical Test*

Mechanical test was carried out at room temperature by using a homemade tensile testing machine of cross head speed of 115 mm/min according to ASTM D 412-80 [2013]. The true stress (σ) and true strain (ε) true strain were calculated according to the Eq. (1) and Eq. (3) [Proulx (2011); Kaufman and Falcetta (1977)] respectively:

$$\sigma = \frac{F}{A_0}\lambda \, . \tag{1}$$

where F is the applied force, A_0 is the initial cross-sectional area of the sample and λ is the elongation which is;

$$\lambda = \frac{l}{l_0} \, . \tag{2}$$

$$\varepsilon = \ln(\lambda). \tag{3}$$

where l is the length of sample under stress while l_0 is the initial length of sample.

2.4. *Hardness Testing*

The hardness studied by NT-6510 Shore Hardness Tester for five specimens of each sample, each of them was disc of 3 cm diameter and 1.2 cm thick.

3. Results and Discussion

3.1. *NS blends*

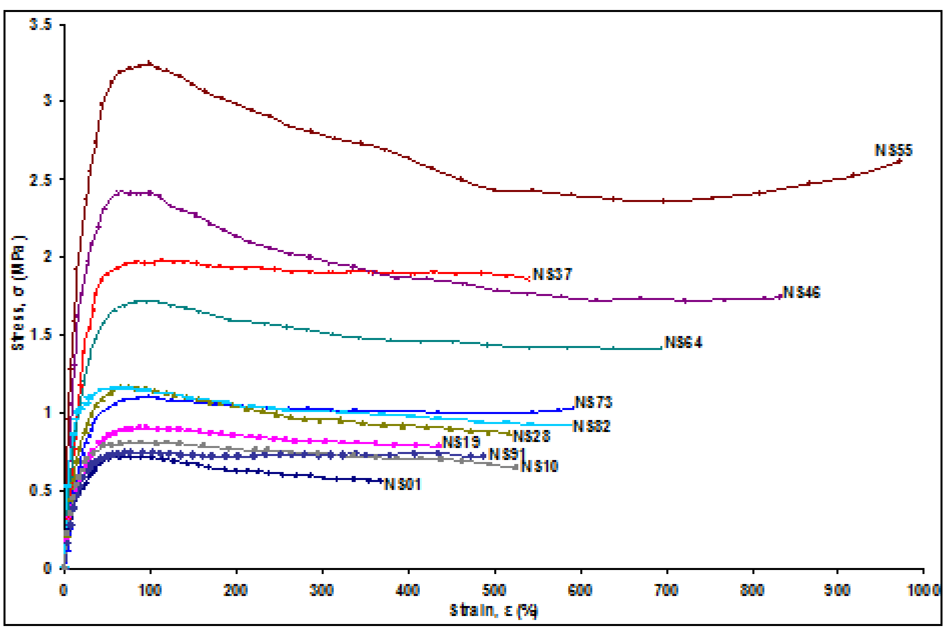

Fig. 1. Stress-strain characteristics for NS blends.

Figure 1 shows the stress-stain curves for NS blends, which report an optimum value at the ratio 50 phr of NR and 50 phr of SBR. This result is also achieved from the values of tensile strength and elongation at break which presented in Fig. 2. These results were found to be in good agreement with Hassan *et al.* [2009].

Journal of. Modern Trends in Physics Research
Online ISSN 2636-4220
DOI: 10.19138/mtpr/(14)65-72
Accepted: 2014-12-19

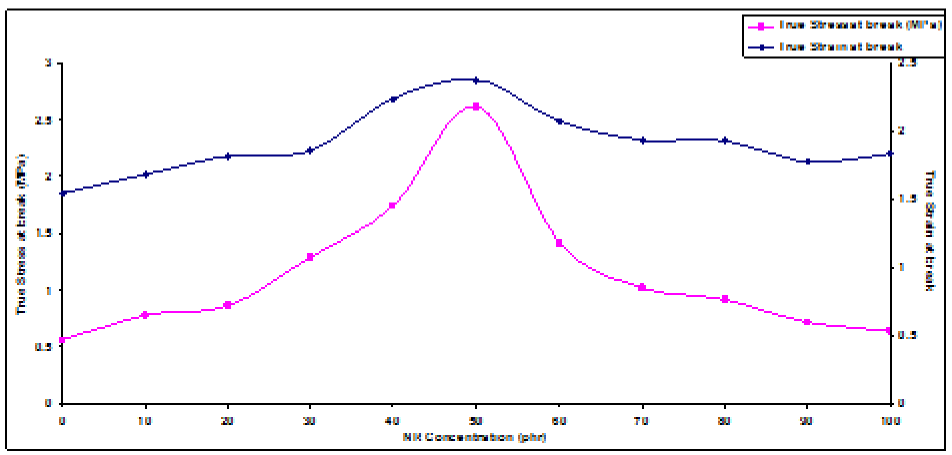

Fig. 2. True stress at break and true strain at break versus NR content for NS blends.

The modulus of elasticity, *E* (Table 3) shows a maximum value for NS55 blend which is in good agreement with the above data.

Table 3. The modulus of elasticity (*E*) of the NS blends.

Sample	NS01	NS19	NS28	NS37	NS46	NS55	NS64	NS73	NS82	NS91
NR (phr)	0	10	20	30	40	50	60	70	80	90
E (MPa)	4.92	5.15	7.20	10.48	13.80	17.73	9.10	5.65	5.37	4.92

The hardness study reports linear decrease of shore A value by negative slope of 0.17 as increasing the NR content in the blend as shown in Fig. 3. In construct to the nature of NR which resists mechanical deformation and enhances blend strength; at which SBR increases the values of hardness of blend quit to its 60% than the pure NR sample.

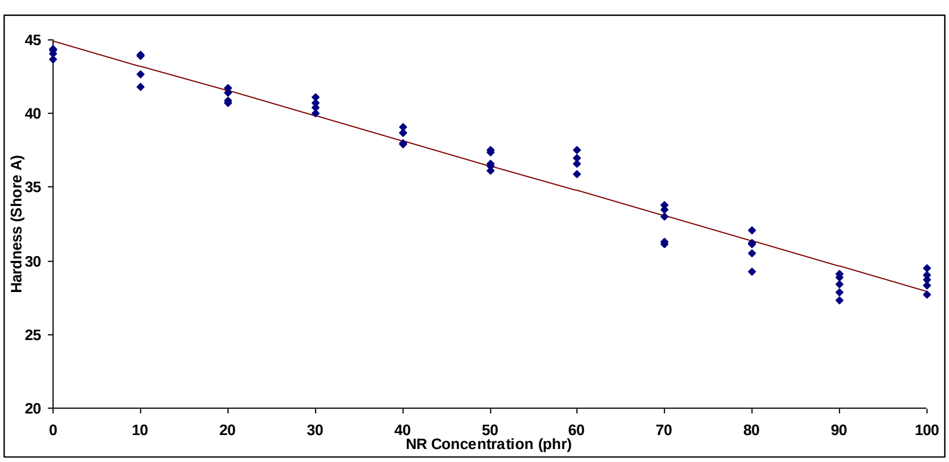

Fig. 3. Hardness versus NR concentration for NS blends.

Journal of. Modern Trends in Physics Research
Online ISSN 2636-4220
DOI: 10.19138/mtpr/(14)65-72
Accepted: 2014-12-19

According to the previous results, the optimum strengthen blend is NS55, then we introduced carbon black with this blend.

3.2. *NS55N2 samples*

Figure 4 shows stress-strain characteristics for NS55N2 samples. It is noticed that, the addition of carbon black results in a marked increase of tensile strength and elongation at break values. The closed inspection of the values presented in Figs 1, 4 show a jump of about ten times of true stress from 2.5 MPa in NS55 to about 25 MPa in carbon filled blend. Sample NS55N2L40 exhibits the maximum values of true stress and true strain as shown in Fig. 5.

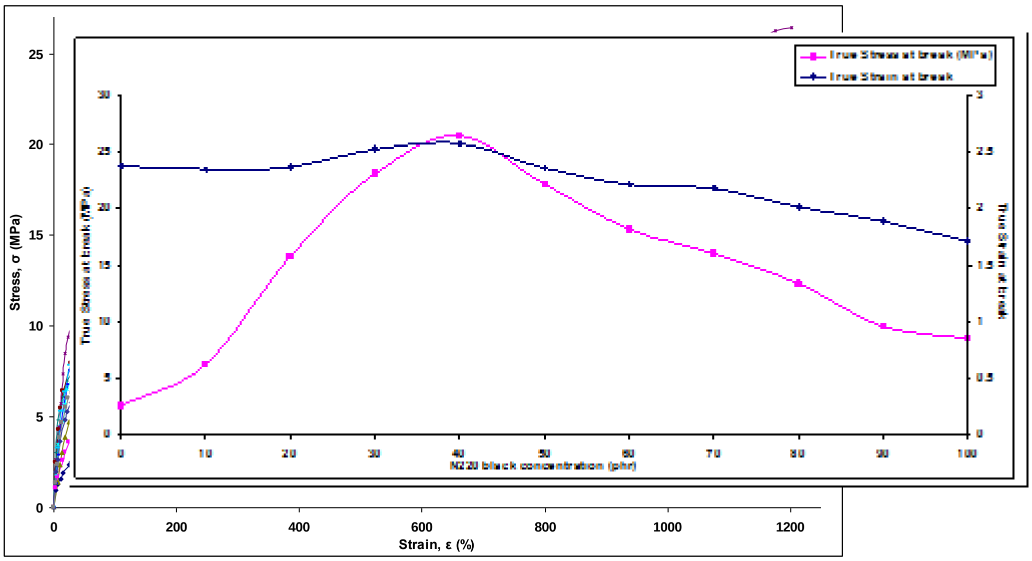

Fig. 4. Stress-strain characteristics for NS55N2 blends.

Fig. 5. True stress at break and true strain at break versus N220 black concentration for NS55N2 samples.

Table 4 shows the modulus of elasticity (*E*) and the shore hardness A for NS55N2 samples.

Table 4. The modulus of elasticity (E) and shore hardness A for NS55N2 samples.

Sample	N220 content (phr)	*E* (MPa)	Shore A
NS55	0	17.73	36.46
NS55N2L10	10	26.23	42.17
NS55N2L20	20	31.81	47.88
NS55N2L30	30	48.48	53.60
NS55N2L40	40	69.23	59.31
NS55N2L50	50	54.89	65.02
NS55N2L60	60	58.27	70.73
NS55N2L70	70	52.90	76.45
NS55N2L80	80	60.43	82.16
NS55N2L90	90	48.78	87.87
NS55N2L100	100	50.01	93.58

Journal of. Modern Trends in Physics Research
Online ISSN 2636-4220
DOI: 10.19138/mtpr/(14)65-72
Accepted: 2014-12-19

It is noticed that, the values of shore hardness A increase approximately by linear relation of slope 0.57 to reach about 2.5 of its initial value at 100 phr of black content. The peak value of *E* at 40 phr of N220 confirms the above obtained results.

3.3. *Data modeling*

Mooney and Rivlin statistical polymer model of Gaussian articulated segmental chain with links lead to an equation which may be written as:

$$\sigma(\lambda) = C_1\left(\lambda^2 - \frac{1}{\lambda}\right) + C_2\left(\lambda - \frac{1}{\lambda^2}\right). \tag{4}$$

This relation between true stress (σ) and elongation ($\lambda=\varepsilon+1$) should be applied to Gaussian region of σ-λ plot, and we can get this region by rewrite Eq. (4) as:

$$\sigma \Big/ \left(\lambda - \frac{1}{\lambda^2}\right) = C_1\lambda + C_2. \tag{5}$$

Plotting the relation between $\sigma \Big/ \left(\lambda - \frac{1}{\lambda^2}\right)$ and λ results in a straight line of slope C_1.

$$C_1 = NkT. \tag{6}$$

where N is the number of effective plastic chains per unit volume; k is Boltzmann's constant, T the absolute temperature. Fig. 6 shows Eq. (5) for three samples namely NS01, NS55, and NS10. The dashed lines represent the straight-line fitting in Gaussian region in range about 1.5~2.5 of elongation.

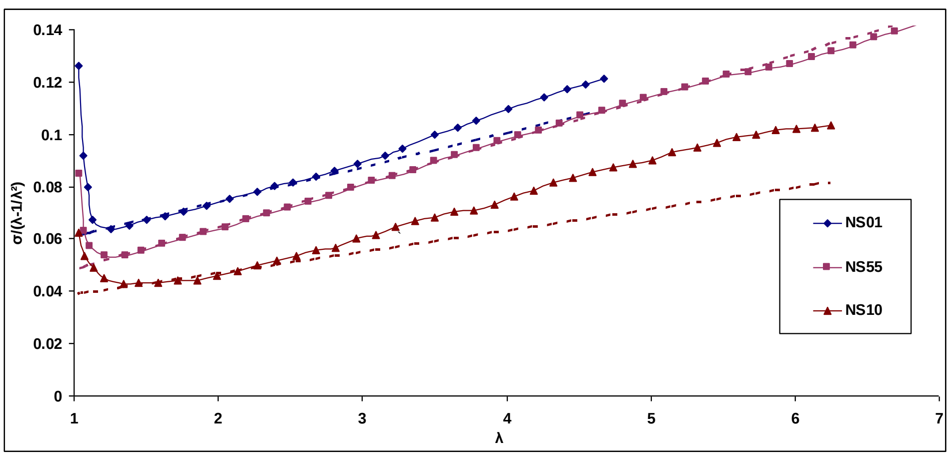

Fig. 6. Relation between $\sigma \Big/ \left(\lambda - \frac{1}{\lambda^2}\right)$ and λ for three selected NS samples.

Journal of. Modern Trends in Physics Research
Online ISSN 2636-4220
DOI: 10.19138/mtpr/(14)65-72
Accepted: 2014-12-19

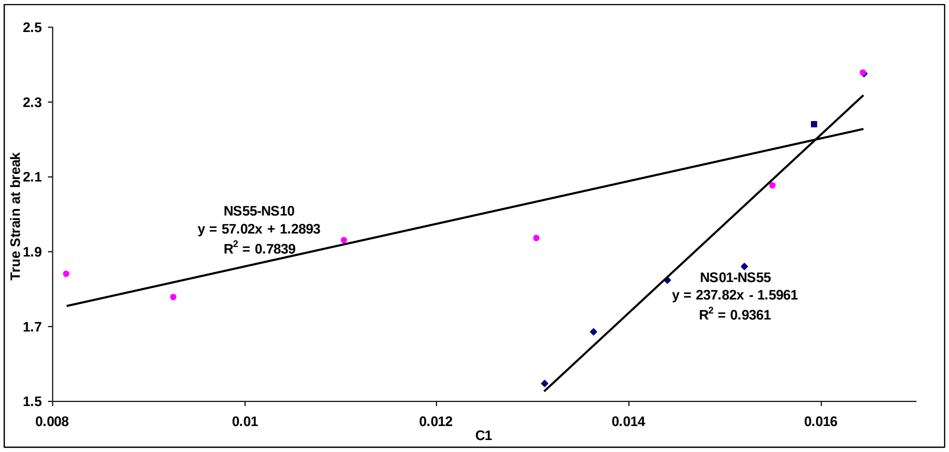

Fig. 7. Constant C_1 versus true strain at break for NS samples.

By using the above model, the constants C_1 and C_2 were calculated and listed in table 5 beside the correlation coefficient R^2 value for the fitting.

Table 5. The constants C_1 and C_2 for NS samples.

	NS01	NS19	NS28	NS37	NS46	NS55	NS64	NS73	NS82	NS91	NS10
C_1 ($\times 10^3$)	13.13	13.63	14.4	15.2	15.94	16.45	15.51	13.04	11.05	9.27	8.17
C_2 ($\times 10^3$)	47.74	44.1	41.2	39	36.7	34.6	33.2	32.3	31.7	31.1	30.42
R^2	0.976	0.881	0.986	0.97	0.991	0.997	0.992	0.986	0.96	0.89	0.878

Figure 7 shows strong correlation between the true strain at break and the shear modulus C_1 for NS samples. It seems that the NR concentrations for the prepared samples are classified into two ranges. The first sub-range is for samples NS01-NS55 gives correlation coefficient 0.885 using least square method. The phr concentrations of the samples NS55-NS10 are in the second sub-range and show a strong correlation with a correlation coefficient 0.967.

However, the shear modulus is determined from fitting of the Gaussian region of stress-strain curve for each sample (λ=1.2~3) the correlations in Fig. 7 give us information about the strains at break.

4. Conclusions

It may be concluded that, the NR/SBR blend exhibits optimum values of tensile strength and elongation at break at the equal ratios of rubbers (50NR/50SBR). The incorporation of this blend with carbon black N220 enhances the mechanical properties. N220 black carbon defines its own optimum at 40 phr.

The theoretical model Mooney-Rivlin was applied to the NR/SBR blends and shows the maximum number of links appears for blend which has two equal ratios of rubbers in good agree to experimental data.

References

Alsuhaiqi, H. N. M., El-Gamel, A. A., Khairy, S. A. and Hassan, H. H. (2014) Effect of compression on the electrical resistivity of EPDM/NBR rubber blends filled with different types of carbon black. *Nat Sci.*, **12(8)**: 154–161.

An, J. E. and Jeong, Y. G. (2013), Structure and electric heating performance of graphene/epoxy composite films. *Eur. Polym. J.*, **49(6)**: 1322–1330.

ASTM D 3182 (2012) Standard Practice for Rubber-Materials, Equipment, and Procedures for Mixing Standard Compounds and Preparing Standard Vulcanized Sheets.

ASTM D 412-80 (2013) Standard Test Methods for Vulcanized Rubber and Thermoplastic Elastomers-Tension.

El-Lawindy, A.M.Y. (2002) Static Deformation of Low Structure HAF Black-Loaded (SBR+NR) Rubber Blend. *Egypt. J. Sol.*, **25**: 93–101.

Flory, P.J. (1953) Principle of Polymer Chemistry. *Univ. Press Ithaca. N.Y.*.

Geyou, A., Quanli, H. and Myung-Soo, K. (2008) Properties of Activated Carbon Blacks Filled SBR Rubber Composites. *Carbon Letters*, **9**: 115–120.,

Guth, E. (1945) Theory of Filler Reinforcement. *J. Appl. Phys.* **16**: 20–25.

Hajji, P., David, L., Gerard, J. F., Pascault, J. P. and Vigier, G. (1999) Synthesis, Structure, and Morphology of Polymer–Silica Hybrid Nanocomposites Based on Hydroxyethyl Methacrylate. *J. Polym. Sci. Polym. Phys.*, **37(22)**: 3172–3187.

Hassan, M. M., Abd El-Megeed, A. A. and Maziad, N. A. (2009) Evaluation of Curing and Physical Properties of NR/SBR Blends Using Radiation-Grafting Copolymer. *Polymer Composites*, **30(6)**: 743–750.

James, H.M. and Guth, E. (1943) Theory of the Elastic Properties of Rubber. *J. Chem. Phys.*, **11**: 455–480.

Kaufman, H.S. and Falcetta, J. J. (1977) Introduction to Polymer Science and Technology. *John Wiley and Sons, Inc., N. Y.*

Mooney, M., (1940) A theory of large elastic deformation. *J. App. Phys.*, **11**: 582–591.

Nair, T.M., Kumaran, M.G. and Unnikrishnan, G. (2004) Mechanical and Aging Properties of Cross-Linked Ethylene Propylene Diene Rubber/Styrene Butadiene Rubber Blends. *J. Appl. Polym. Sci.*, **93**: 2606–2621.

Proulx, T. (2011) Dynamic Behavior of Materials. *Conference Proceedings of the Society for Experimental Mechanics Series*, **1**: 361–368

Rivlin, R. S. (1948) Large elastic deformation of isotropic materials. *Phil. Trans. Royal Soc. London*, **A240**: 459–491.

Vand, V. (1948) *J. Phys. Colloid. Chem.* **52**: 277.

Wall, F.T. (1943) Statistical Thermodynamics of Rubber. III. *J. Chem. Phys.*, **11**: 527–530.

Zhou, X. W., Zhu, Y. F. and Liang, J. (2007), Preparation and properties of powder styrene–butadiene rubber composites filled with carbon black and carbon nanotubes. *Materials Research Bulletin*, **42(3)**: 456–464.